SPECIAL REPORT 96-19

Resilient Modulus Testing of Materials from Mn/ROAD, Phase 1

Richard L. Berg, Susan R. Bigl, Jeffrey A. Stark
and Glenn D. Durell

September 1996

Abstract: The U.S. Army Cold Regions Research and Engineering Laboratory (CRREL) conducted resilient modulus tests on materials from the Mn/ROAD test site for the Minnesota Department of Transportation. Materials tested included samples of the lean clay subgrade at the site and the two extreme grades of base designed specifically for Mn/ROAD. Some specimens were tested in both frozen and subsequently "thawed" conditions; others were tested at room temperature without ever having been frozen. Researchers performed linear regression analysis on the data to develop equations that predict frozen modulus based on unfrozen water content and unfrozen modulus based on stress, degree of saturation and density. We also reanalyzed data from two previously tested materials. CRREL can use the study's equations in the Mechanistic Pavement Design and Evaluation Procedure under development at CRREL to predict estimated damage in some Mn/ROAD test sections.

How to get copies of CRREL technical publications:

Department of Defense personnel and contractors may order reports through the Defense Technical Information Center:

DTIC-BR SUITE 0944
8725 JOHN J KINGMAN RD
FT BELVOIR VA 22060-6218
Telephone 1 800 225 3842
E-mail help@dtic.mil
msorders@dtic.mil
WWW http://www.dtic.dla.mil/

All others may order reports through the National Technical Information Service:

NTIS
5285 PORT ROYAL RD
SPRINGFIELD VA 22161
Telephone 1 703 487 4650
1 703 487 4639 (TDD for the hearing-impaired)
E-mail orders@ntis.fedworld.gov
WWW http://www.fedworld.gov/ntis/ntishome.html

A complete list of all CRREL technical publications is available from:

USACRREL (CECRL-TL)
72 LYME RD
HANOVER NH 03755-1290
Telephone 1 603 646 4338
E-mail techpubs@crrel.usace.army.mil

For information on all aspects of the Cold Regions Research and Engineering Laboratory, visit our World Wide Web site:
http://www.crrel.usace.army.mil

Special Report 96-19

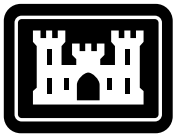

US Army Corps of Engineers
Cold Regions Research & Engineering Laboratory

Resilient Modulus Testing of Materials from Mn/ROAD, Phase 1

Richard L. Berg, Susan R. Bigl, Jeffrey A. Stark
and Glenn D. Durell

September 1996

Prepared for
MINNESOTA DEPARTMENT OF TRANSPORTATION

PREFACE

This report was prepared by Dr. Richard L. Berg, Research Civil Engineer (retired), Susan R. Bigl, Research Physical Scientist, Jeffrey A. Stark, Supervisory Civil Engineering Technician, Civil and Geotechnical Research Division, Research and Engineering Directorate, and Glenn D. Durell, Engineering Technician, Engineering Resources Branch, Technical Resources Center, U.S. Army Cold Regions Research and Engineering Laboratory (CRREL), Hanover, New Hampshire.

This work was funded through Agreement 64632, Task Order 1 with the Minnesota Department of Transportation (Mn/DOT) and a Construction Productivity Advancement Research (CPAR) project between Mn/DOT and CRREL. The authors thank George Cochran of the Minnesota Road Research Project and Dr. Vincent Janoo of CRREL for technically reviewing the manuscript of this report.

This report covers results from the subgrade and two base materials available in 1990 and is considered Phase 1. Additional materials were manufactured later and are described separately as Phase 2 results.

The information reported here is the result of work done by a team of CRREL personnel whose efforts we greatly appreciate. Arthur Peacock, Brian Charest, and David Carbee were all involved in molding, freezing, and milling the specimens. Dale Bull conducted some of the resilient modulus testing. Brian Charest characterized the water content and density subsequent to resilient modulus testing.

CONTENTS

ILLUSTRATIONS

TABLES

EXECUTIVE SUMMARY

Laboratory resilient modulus tests were conducted on pavement materials from the Minnesota Road Research Project (Mn/ROAD) to characterize their behavior under seasonal frost conditions, and to provide input necessary for modeling the materials with the Mechanistic Pavement Design and Evaluation Procedure under development at CRREL. Results of other tests to characterize their physical properties (grain-size distribution, specific gravity, Atterberg limits, organic content, hydraulic properties, and compaction) as well as tests more specifically related to freeze/thaw processes (frost susceptibility and unfrozen moisture content) are reported separately (Bigl and Berg 1996a).

The materials reported on here include two samples of the clay subgrade from beneath the Mn/ROAD site (the high-heaving sample 1206 and the low-heaving sample 1232) and the two bases with the least (class 6 special) and greatest (class 3 special) amounts of the fine fraction. When this testing was performed, the two bases with intermediate amounts of fines (class 4 special and class 5 special) were unavailable. However, to conduct subsequent modeling with the Mechanistic Pavement Design and Evaluation Procedure, it was necessary to approximate their behavior using properties of similar materials. Therefore, this report includes modulus test results conducted previously on materials most closely matching the specified size gradations of the class 4 and class 5 special subbases. A subbase from taxiway A at the Albany, New York, airport (Cole et al. 1987) substituted for the class 4 special subbase; dense-graded stone, from a Winchendon, Massachusetts, test site (Cole et al. 1986) substituted for the class 5 special.

Specimens of the materials were molded at a specified moisture/density condition and then saturated. Once saturated, they were frozen with an open system, allowing movement of any additional water required to the freezing front. Specimens were tested using repeated load triaxial procedures at a matrix of applied confining and deviator stresses. Testing was first conducted at three temperatures below freezing, and then specimens were allowed to thaw in the triaxial device and subsequently retested in a thawed, saturated state. The same specimens of the base materials were subsequently tested at room temperature under several moisture contents created by drawing a suction at the base of the specimen. To obtain unfrozen data for the subgrade materials, different specimens were molded to specific moisture conditions and tested at room temperature without ever having been frozen. A different testing machine was used for the unfrozen specimens of the 1206 subgrade than for all other testing. It was discovered after testing was complete that these data include a calibration error of unknown magnitude that produced moduli about an order of magnitude too high.

All materials exhibited a two to three order of magnitude increase in resilient modulus at subfreezing temperatures of –2°C and lower. The modulus of all of the materials was stress dependent and also showed a lower magnitude increase as the degree of saturation decreased. For the materials where a variety of densities were tested, modulus was also dependent on density.

The resilient modulus data from the materials tested in this study were analyzed using statistical regression techniques. Data from the two previously tested materials were also reanalyzed. In the regression analysis, the resilient modulus was the

dependent variable. For the frozen condition, a function of the unfrozen water content was the independent variable; for the thawed/unfrozen condition, various forms and combinations of stress, density, and degree of saturation were the independent variables. The equations resulting from this analysis have been subsequently utilized in the CRREL Mechanistic Pavement Design Procedure to predict estimated damage in some of the test sections at Mn/ROAD. Results of the modeling effort are described in Bigl and Berg (1996b). Another report in this series (Bigl and Berg 1996c) summarizes all the testing and modeling results.

Resilient Modulus Testing of Materials from Mn/ROAD, Phase 1

RICHARD L. BERG, SUSAN R. BIGL, JEFFREY A. STARK AND GLENN D. DURELL

INTRODUCTION

This report describes resilient modulus testing that CRREL conducted on materials from Mn/ROAD for the Minnesota Department of Transportation (Mn/DOT). Results of other tests to determine physical and behavioral characteristics are reported separately (Bigl and Berg 1996a). The materials tested included samples of the subgrade at the site and the two extreme grades of base and subbase designed especially for Mn/ROAD: class 6 special, a clean base material, and class 3 special, a subbase material with a high percentage of fines. Some specimens were tested in both frozen and subsequently thawed conditions; others were tested at room temperature without ever having been frozen. Two intermediate grades of base—class 4 special, class 5 special, and an R-70 subgrade—were manufactured later and results of their testing are described in Berg (in prep.).

The resilient modulus tests were conducted using repeated-load triaxial test procedures described by Cole et al. (1985, 1986). The tests involve applying a confining pressure to a cylindrical specimen within a cell, while also applying a cyclical loading of a deviator stress to the top end of the specimen. The resilient modulus is defined as the applied deviator stress divided by the recovered strain upon unloading (the resilient axial strain) for a representative loading cycle.

Linear regression analyses were performed on the resilient modulus data from the materials tested in this study. Data from two previously tested materials that are similar to the intermediate grades of base/subbase materials (class 4 special and class 5 special) that will be used at Mn/ROAD were reanalyzed. In the regression analysis, the resilient modulus was the dependent variable and various forms and combinations of stress, density, and degree of saturation were the independent variables. The equations resulting from this analysis have been subsequently utilized in the mechanistic pavement design procedure under development at CRREL to predict estimated damage that would occur in some of the Mn/ROAD test sections. Results of the modeling effort are described in Bigl and Berg (1996b).

METHODS

Materials/conditions tested

The materials tested included the two extreme grades of base—class 6 special and class 3 special, and the 1206 and 1232 subgrade samples that represent, respectively, the high- and low-heaving sandy lean clay (CL) subgrades. Specimens of the base materials were tested in a frozen saturated condition at three temperatures (class 6 special at –5.0°, –3.0°, and –2.0°C; class 3 special at –7.0°, –5.0°, and –2.0°C). The same specimens were subsequently warmed to above freezing and tested again at various thawed conditions in a range of moisture levels created by drawing a suction at the base of the specimens. Frozen, saturated subgrade specimens were similarly tested at three temperatures below freezing (–7.0°, –5.0°, and –2°C) and also tested subsequently in a thawed, saturated state at room temperature. To acquire above-freezing resilient modulus data for the subgrade samples at various moisture contents, we molded specimens to specified conditions and

Table 1. Samples tested for resilient modulus.

	Condition		
Material	*Frozen*	*Thawed*[*]	*Never frozen*
Sandy lean clay subgrade (CL)			
1206 (high heave)	4	4[†]	24
1232 (low heave)	8	8[†]	18
Class 3 stockpile	5	4[**]	
Class 6 stockpile	7	6[**]	
Total	24		42

[*] Same samples were tested in the frozen and thawed condition
[†] Samples tested only in the thawed, undrained condition
[**] Thawed samples were tested at several moisture contents

tested at room temperature. We refer to these as a "never frozen" specimens. Specimens of the low-heaving subgrade (1232) included replicates of various moisture contents at a single density; for the high-heaving subgrade (1206), replicates were made with variation in both moisture and density conditions. A total of 66 specimens were prepared (Table 1).

Specimen preparation

The specimen size used for the subgrades and the class 3 special subbase was 5.1 cm (2 in.) diam. and 12.7 cm (5 in.) long. The coarser class 6 special material was tested using specimens measuring 15.2 cm (6 in.) in diam. and 39.4 cm (15.5 in.) in length. Gradation curves and other physical properties of these materials are in Bigl and Berg (1996a).

Specimens that were tested in frozen/thawed conditions were first molded at the specified moisture/density condition, which was usually at optimum as determined from the compaction testing. The subgrade specimens were compacted with a CE-12 (Standard Proctor) compaction effort, while the class 3 special and class 6 special were compacted with a CE-55 (Modified Proctor) effort to approximate anticipated in-situ conditions (Table 2). The specimens were then prepared in a manner similar to the procedure used in the frost susceptibility test (Chamberlain 1987). They were set on a special base with a porous stone and saturated from the base up with a constant head water supply. Once saturated, the specimens and their porous-stone bases were positioned with two other special plates that could circulate temperature-regulated fluid at the top and bottom. The bottom porous plate allowed movement of any additional water required for open system freezing. The fluid temperatures were set to allow freezing from the top down at the rate of about 2.5 cm (1 in.) per day. The specimens were frozen with a surcharge of 3.4 kPa (0.5 lb/in.^{2}) placed on the upper cold plate; this weight simulates the weight of a 15.2-cm (6-in.)-thick asphalt concrete pavement surface.

After freezing was complete, the specimen ends were trimmed to assure that they were smooth and flat. For the subgrade specimens, this was done by milling the ends flat. For the base and subbase materials, we made a slurry of fine material that was placed in custom-made equipment similar to that used for capping concrete specimens with molten sulfur. The slurry was then frozen to the ends of the specimen and milled flat and smooth.

Subgrade specimens tested at room temperature without being frozen were molded at the specified moisture/density levels, trimmed with a knife, and tested immediately. For the Sample 1232 subgrade, the density was held constant at about 1.76 Mg/m^3 (110 lb/ft^3) and the moisture content was varied from 13% to a saturated value of 20%, by weight (Table 2). For the 1206 subgrade, specimens were prepared at three compactive efforts, with moisture contents intended to be at three conditions: optimum, 2% above optimum, and 2% below optimum (Table 2).

Test procedures

The resilient modulus tests were conducted using repeated-load triaxial test procedures, the details of which are described in reports by Cole et al. (1985 and 1986). Testing was accomplished in triaxial cells that were constructed to accommodate the instrumentation used to monitor load and deformation (Fig. 1). Separate cells were used for the 5.1- and 15.2-cm (2- and 6-in.)-diam. specimens. The triaxial cells were designed so that the cell base could be removed from the rest of the major cell components. In this way, a specimen could remain on its base while the remainder of the assembly was used on other specimens in a rotating sequence. A miniature, high-precision load cell mounted in the

triaxial cell on the loading piston was used to monitor the load applied to the specimen.

The axial deformation was monitored using two LVDTs, or linear variable displacement transducers, mounted on hinged arms. The LVDT assemblies were mounted on two circumferential rings clamped around the specimen. Radial deformation was also monitored using three noncontacting multi-VITs (variable impedance transducers) spaced evenly around the specimen at its midpoint. These pointed at small aluminum foil targets positioned on the specimen.

Table 2. Resilient modulus samples tested.

Subgrade 1206			Subgrade 1232		
No.	*Dry density Mg/m³ (lb/ft³)*	*Water content (% by wt)*	*No.*	*Dry density Mg/m³ (lb/ft³)*	*Water content (% by wt)*
Never frozen			**Never frozen**		
5K Compactive effort*			CE 55 Compactive effort		
18A	1.77 (110.3)	13.7	14A	1.76 (109.8)	13.1
18B	1.72 (107.4)	15.9	14B	1.78 (111.4)	12.9
18C	1.69 (105.3)	16.1	14C	1.78 (111.4)	13.0
21B	1.70 (106.4)	19.7	15A	1.78 (111.0)	14.4
21C	1.70 (106.1)	17.3	15B	1.77 (110.8)	14.1
			15C	1.79 (112.0)	13.8
22A	1.69 (108.4)	19.0	15D	1.77 (110.3)	14.3
22B	1.73 (108.0)	19.1			
22C	1.74 (108.6)	18.3	16A	1.76 (109.9)	15.7
			16B	1.75 (109.0)	15.7
CE 12 Compactive effort			16C	1.76 (110.0)	15.6
16A	1.69 (105.6)	13.5	16D	1.77 (110.7)	15.5
16B	1.67 (104.4)	14.1			
16C	1.89 (118.1)	14.3	18A	1.75 (109.3)	17.5
			18B	1.75 (109.5)	17.5
18A	1.69 (105.4)	17.4	18C	1.76 (109.9)	17.5
18B	1.71 (106.9)	15.9	18D	1.76 (110.0)	17.2
18C	1.72 (107.3)	15.9			
			S1	1.70 (106.1)	20.5
20A	1.69 (105.8)	18.5	S2	1.68 (104.7)	21.3
20C	1.70 (106.1)	17.8	S3	1.70 (106.3)	20.3
CE 55 Compactive effort			**Frozen/thawed (saturated)**		
13A	1.74 (108.5)	11.0	CE 12 Compactive effort		
13B	1.68 (105.1)	10.6	M4-1A	1.73 (107.8)	18.9
			M4-1B	1.72 (107.5)	18.8
15A	1.88 (117.3)	13.9	M4-2A	1.71 (106.6)	19.3
15B	1.82 (113.9)	13.4	M4-2B	1.72 (107.6)	18.3
15C	1.85 (115.7)	13.5			
			M6-1A	1.69 (105.6)	18.9
17A	1.82 (113.9)	14.9	M6-1B	1.72 (107.1)	19.2
17B	1.86 (116.1)	14.9	M6-3A	1.68 (104.7)	19.4
17C	1.84 (114.9)	14.4	M6-3B	1.68 (104.7)	20.2
Frozen/thawed (saturated)					
CE 12 Compactive effort					
M5-1A	1.71 (106.5)	22.6			
M5-1B	1.67 (104.1)	24.1			
M5-2A	1.68 (104.6)	23.4			
M5-2B	1.70 (106.0)	22.8			

* 5K compactive effort = 5,000 ft-lb/ft^3 applied in layers similar to the CE 12 and CE 55 test methods.

Table 2 (cont'd). Resilient modulus samples tested.

Class 3 Subbase		
No.	*Dry density Mg/m³ (lb/ft³)*	*Water content (% by wt)*
Thawed		
CE 55 Compactive effort		
Class 3-1	2.11 (131.5)	7.2
	2.12 (132.1)	3.3
	2.12 (132.3)	0.8
Class 3-2R	2.13 (132.7)	5.1
	2.12 (132.6)	3.2
	2.12 (132.3)	0.8
Class 3-3	2.09 (130.4)	8.3
	2.10 (131.2)	6.7
	2.10 (130.9)	2.1
	2.10 (131.4)	1.4
Class 3-4	2.08 (129.6)	9.3
	2.09 (129.8)	7.9
	2.09 (130.5)	4.0
	2.10 (131.0)	2.4
Frozen		
Class 3-1	2.06 (128.3)	7.6
Class 3-2	2.09 (130.7)	6.2
Class 3-3	2.03 (126.5)	9.3
Class 3-4	2.02 (125.8)	10.1

Class 6 Base Course		
No.	*Dry density Mg/m³ (lb/ft³)*	*Water content (% by wt)*
Thawed		
CE 55 Compactive effort		
Class 6-2	2.08 (130.0)	9.6
	2.08 (130.0)	6.0
Class 6-3	2.06 (128.4)	10.1
	2.06 (128.4)	8.9
	2.09 (130.7)	7.3
Class 6-4	2.09 (130.6)	9.5
	2.09 (130.6)	7.5
	2.14 (133.8)	7.2
	2.14 (133.8)	6.5
Class 6-5	2.06 (128.7)	9.3
	2.06 (128.7)	7.1
	2.05 (128.2)	5.1
	2.05 (128.2)	4.8
	2.10 (131.0)	2.4
Class 6-6	2.13 (133.1)	8.9
	2.18 (136.0)	4.9
	2.18 (136.0)	4.4
	2.14 (133.3)	1.6
	2.14 (133.8)	0.7
Class 6-9	2.10 (134.2)	8.2
	2.08 (136.2)	7.0
	2.06 (136.2)	6.1
	2.09 (136.2)	5.4
	2.17 (135.3)	4.0
	2.17 (135.3)	1.4
	2.18 (136.3)	0.5
Frozen		
Class 6-1	2.10 (130.9)	9.4
Class 6-2	2.08 (130.0)	9.6
Class 6-3	2.06 (128.4)	10.1
Class 6-4	2.09 (130.6)	9.5
Class 6-6	2.13 (133.1)	8.9
Class 6-9	2.15 (134.2)	8.2

The specimen was first positioned on one of the cell bases with an aluminum cap placed on top. It was then encased in a thin latex membrane with O-rings at the top and bottom. The aluminum foil targets for the multi-VITs were secured to this first membrane, then a second membrane was placed over the first to protect the multi-VITs. The remainder of the instrumentation was then attached to the specimen and cell in the necessary positions. Once the cell was assembled, the specimen was tested in repeated-load triaxial compression using a closed-loop, electrohydraulic testing machine.

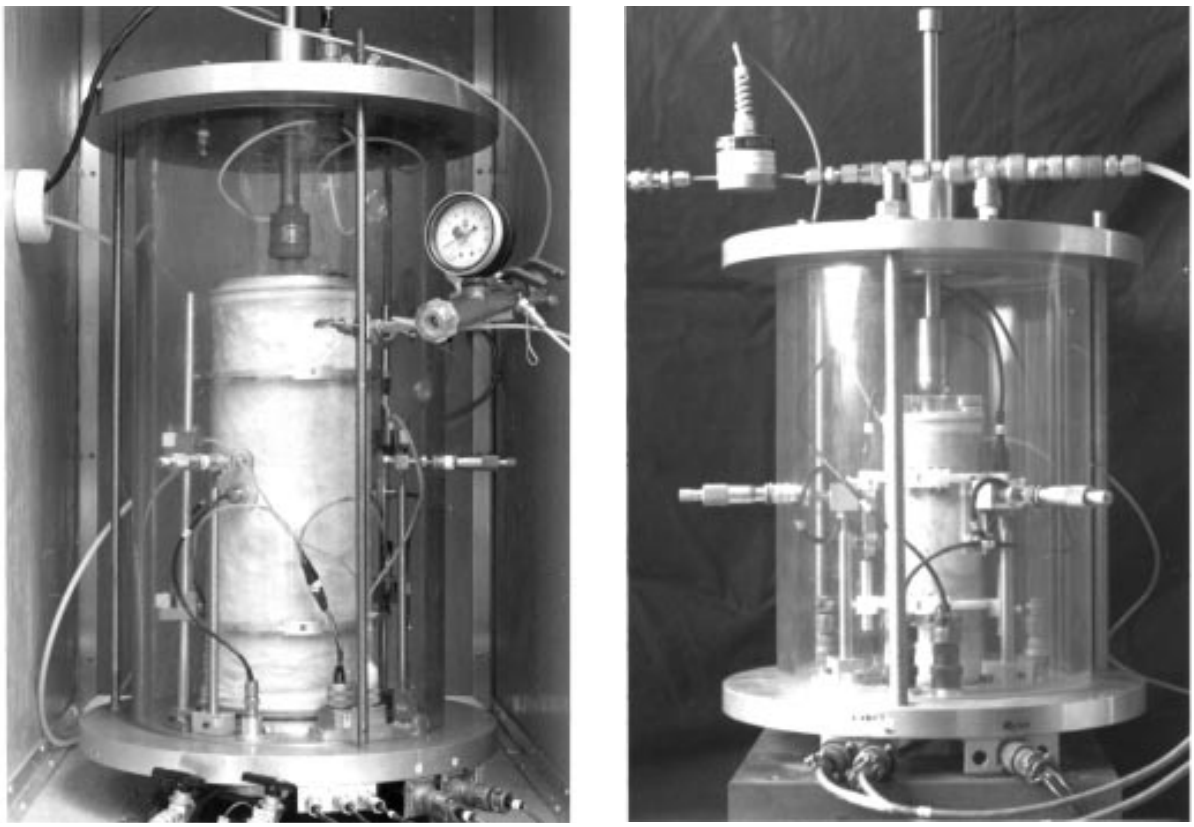

Figure 1. Examples of triaxial cells. Cells for 15.2- (left) and 5.1-cm-diam. specimens.

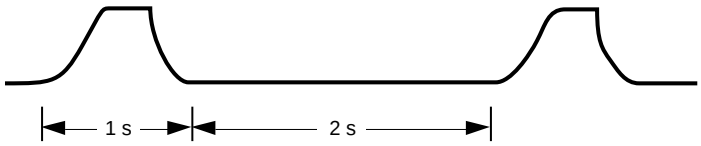

Figure 2. Waveform used in Mn/ROAD resilient modulus testing.

For this study, the waveform used to apply the cyclic deviator stress was the waveform shown in Figure 2. The pulse length is approximately 1 second with 2 seconds between pulses. Table 3a illustrates the sequence of stress conditions applied to the unfrozen specimens, whether thawed or never frozen. We applied only the stress combinations that would avoid excessive permanent strains in the specimens (5% decrease in axial length), depending on the moisture condition and estimated available strength. The frozen specimens were tested holding the confining pressure constant at 69 kPa (10 lb/in.^{2}) and varying the deviator stress as shown in Table 3b. The frozen specimens were tested at three temperatures: class 6 special specimens were tested at approximately –5.0°, –3.0°, and –2.0°C (23.0°, 26.6° and 28.5°F); all other specimens were tested at –7.0°, –5.0°, and –2.0°C (19.5°, 23.0° and 28.5°F). The cyclical deviator stress was applied at each test point until the resilient axial strain remained a constant value, which occurred at about 70–100 applied cycles.

Once the tests on the frozen specimens were completed, they were allowed to thaw in the triaxial device and subsequently retested in a thawed, saturated state. For the coarser-grained materials, the specimens were then allowed to drain in place, and tested again. Increasing amounts of suction were applied to the base and subbase specimens to bring them to various moisture states, and additional test points were determined.

Previously tested materials

In order to conduct the follow-on modeling of predicted damage at the test sections of the Mn/ROAD facility, resilient modulus characterization was needed for two additional Mn/DOT subbase materials, class 4 special and class 5 special. We looked through CRREL's collection of material

Table 3. Stress conditions of resilient modulus tests in current study.

Confining pressure σ_3, *kPa (lb/in.^{2})*	*Deviator stress* σ_d, *kPa (lb/in.^{2})*	*Stress ratio* (σ_1/σ_3)
a. Thawed or never-frozen specimens		
48.3 (7)	48.3 (7.0)	2.0
48.3 (7)	34.5 (5.0)	1.7
48.3 (7)	27.6 (4.0)	1.6
48.3 (7)	20.7 (3.0)	1.4
48.3 (7)	13.8 (2.0)	1.3
48.3 (7)	6.9 (1.0)	1.1
48.3 (7)	3.4 (0.5)	1.1
27.6 (4)	48.3 (7.0)	2.8
27.6 (4)	34.5 (5.0)	2.3
27.6 (4)	27.6 (4.0)	2.0
27.6 (4)	20.7 (3.0)	1.8
27.6 (4)	13.8 (2.0)	1.5
27.6 (4)	6.9 (1.0)	1.3
27.6 (4)	3.4 (0.5)	1.1
13.8 (2)	34.5 (5.0)	3.5
13.8 (2)	27.6 (4.0)	3.0
13.8 (2)	20.7 (3.0)	2.5
13.8 (2)	13.8 (2.0)	2.0
13.8 (2)	6.9 (1.0)	1. 5
13.8 (2)	3.4 (0.5)	1.3
6.9 (1)	34.5 (5.0)	6.0
6.9 (1)	27.6 (4.0)	5.0
6.9 (1)	20.7 (3.0)	4.0
6.9 (1)	13.8 (2.0)	3.0
6.9 (1)	6.9 (1.0)	2.0
6.9 (1)	3.4 (0.5)	1.5
b. Frozen specimens		
69 (10)	34 (5)	–
69 (10)	69 (10)	–
69 (10)	103 (15)	–
69 (10)	138 (20)	–
69 (10)	207 (30)	–
69 (10)	276 (40)	–
69 (10)	345 (50)	–
69 (10)	483 (70)	–
69 (10)	621 (90)	–
69 (10)	690 (100)	–

Notes:

Thawed samples: each combination of stresses normally used at each moisture condition.

Frozen samples: each combination of stresses normally used at each of three temperatures.

Table 4. Stress conditions of resilient modulus tests—previous study.

Confining pressure σ_3, *kPa (lb/in.^{2})*	*Deviator stress* σ_d, *kPa (lb/in.^{2})*	*Stress ratio* (σ_1/σ_3)
a. Thawed specimens		
6.9 (1)	3.4 (0.5)	1.5
13.8 (2)	6.9 (1.0)	1.5
27.6 (4)	13.8 (2.0)	1.5
48.3 (7)	24.1 (3.5)	1.5
69.0 (10)	34.5 (5.0)	1.5
6.9 (1)	6.9 (1.0)	2.0
13.8 (2)	13.8 (2.0)	2.0
27.6 (4)	27.6 (4.0)	2.0
48.3 (7)	48.3 (7.0)	2.0
69.0 (10)	69.0 (10.0)	2.0
6.9 (1)	10.3 (1.5)	2.5
13.8 (2)	20.7 (3.0)	2.5
27.6 (4)	41.4 (6.0)	2.5
48.3 (7)	72.4 (10.5)	2.5
69.0 (10)	103.4 (15.0)	2.5
b. Frozen specimens		
69 (10)	60 (9)	–
69 (10)	138 (20)	–
69 (10)	207 (30)	–
69 (10)	276 (40)	–
69 (10)	345 (50)	–
69 (10)	483 (70)	–
69 (10)	621 (90)	–
69 (10)	827 (120)	–

types for which resilient modulus data were available and found the two materials that most closely fit Mn/DOT's specifications for size gradation (Fig. 3). A dense-graded stone tested at a cooperative study in Winchendon, Massachusetts, most closely matched the specifications of the class 5 special material; a subbase material from taxiway A at the Albany, New York, airport most closely matched the class 4 special specifications (Bigl and Berg 1996a).

The methods used during the testing of these materials were nearly identical to the methods of this study. Details of the testing procedures for dense-graded stone are described in Cole et al. (1986) and the procedures for Albany taxiway A subbase are in Cole et al. (1987). Both materials were molded into 15.2-cm (6-in.)-diam. specimens in the laboratory from bulk field samples and then

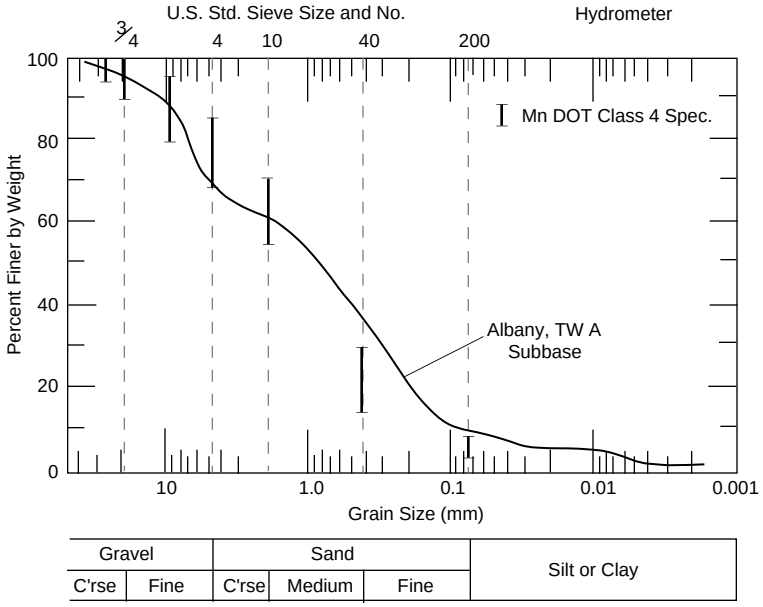

a. Albany, New York, taxiway A subbase/class 4 special subbase.

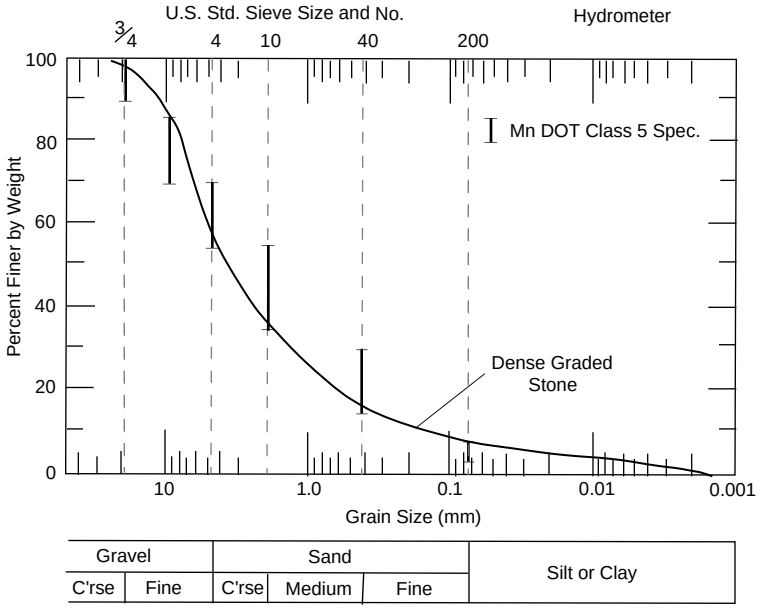

b. Dense-graded stone, Winchendon, Massachusetts/class 5 special subbase.

Figure 3. Comparison of Mn/DOT specifications with size gradations of substitute materials.

frozen from the top down at 2.5 cm (1 in.) per day with open system freezing. This procedure differs from the current study in that the specimens were not saturated prior to freezing. Another difference in this prior testing is the sequence of stresses applied to the specimens (Table 4). In this case also, the stress combinations applied were those that would avoid excessive permanent strains in the specimens (5% axial length shortening).

The previous regression analysis of the resilient modulus data obtained from this earlier testing had been based on characterizing the moisture level of the unfrozen material with the measured moisture tension. The data were reanalyzed using degree of saturation as the indicator of moisture condition.

DATA REDUCTION AND ANALYSIS

For each set of applied deviator and confining stresses, the resilient and permanent axial and ra-

dial strains were recorded, and thus were used to calculate a resilient modulus and Poisson's ratio. The resilient modulus is defined as the applied deviator stress divided by the strain recovered upon unloading for a representative loading cycle, or resilient axial strain. To calculate the resilient axial strain, the measured resilient axial deformation is divided by the gauge length over which it is determined. Poisson's ratio is defined as the recoverable radial strain divided by the recoverable axial strain.

The following data were then tabulated in a spreadsheet: confining stress, deviator stress, resilient axial strain, resilient radial strain, density, and moisture condition or temperature. The tables in Appendix A contain these data along with the calculated results. The equivalent data for the previously tested materials are given in Appendix B. These tables also show the actual stress combinations applied to each specimen.

The frozen and unfrozen data were analyzed separately using statistical regression techniques. The nonlinear form of the equation used to model the resilient modulus was the same in both cases, as given by

$$M_r = K_1 P^{K_2}, \quad (1)$$

where K_1 and K_2 are constants and P is a governing parameter. This equation was linearized by taking the natural log of both sides, resulting in an equation of the form

$$\ln M_r = A_0 + A_1 \ln P, \quad (2)$$

where A_0 and A_1 are constants. To conduct the regression, the natural log of the modulus was set as the dependent variable and the natural log of the governing parameter was set as the independent variable. In this general case,

$$K_2 = A_1 \text{ and } K_1 = e^{A_0}.$$

Frozen

In attempting to represent the frozen data with the general form eq 1, we tried three different governing parameters, all related to the unfrozen water content of the material, w_u. The unfrozen water content present in the materials at various temperatures, expressed in gravimetric form, w_{u-g}, had been determined in earlier characterization tests on the Mn/ROAD materials (Bigl and Berg 1996a). It is related to the temperature in the form

$$w_{u-g} = \alpha/100\ (-T/T_o)^{\beta};\ T < 0°C \quad (3)$$

where w_{u-g} = gravimetric unfrozen moisture content, in decimal form
T = temperature, °C
T_o = 1.0°C
α and β = constants.

Table 5 presents the α and β constants characteristic of each material.

The first governing parameter we tried was w_{u-g}, expressed as a decimal, which had been normalized to the total gravimetric water content in the sample, w_t, also expressed as a decimal. The resulting equation was as follows:

$$M_r = K_1 (w_{u-g}/w_t)^{K_2}. \quad (4)$$

This governing parameter has a good physical basis. When the material is very cold and solidly frozen, there is very little unfrozen water and the ratio w_{u-g}/w_t is a small number (<< 1). When the material is just below the freezing point, w_{u-g}/w_t approaches a value of 1. However, when this form of the equation was used in the mechanistic design procedure (Bigl and Berg 1996b), the calculated amount of total water was often very high, and the ratio of unfrozen water to total water was unreasonably small. Therefore, other relationships were considered.

Table 5. Constants for unfrozen moisture content equations.

Soil	*α*	*β*
Subgrade		
1206	11.085	–0.274
1232	8.121	–0.303
Class 3		
Stockpile	1.497	–0.709
Class 4		
Taxiway A	3.0	–0.25*
Class 5		
Dense stone	2.0	–0.40*
Class 6		
Stockpile	0.567	–1.115

* Values for these materials are estimated

The two other forms that were used to represent the unfrozen water content in the governing parameter of eq 1 were directly related to the unfrozen water content, as follows: 1) w_{u-g}, expressed as a decimal, normalized to a unit unfrozen water content, w_o, of 1.0; and 2) the volumetric unfrozen water content, w_{u-v}, expressed as a decimal, normalized to a unit unfrozen water content, w_o, of 1.0. The volumetric unfrozen water content was determined with

$$w_{u-v} = w_{u-g}\ \gamma_d \tag{5}$$

where γ_d = dry density (Mg/m^3). The resulting equations with these terms substituted as the governing parameter were:

$$M_r = K_1\left(w_{u-g} / w_o\right)^{K_2}$$

$$M_r = K_1\left(w_{u-v} / w_o\right)^{K_2}.$$

In analyzing the frozen resilient modulus data, the value of the governing parameter w_{u-g} / w_t, w_{u-g} / w_o, or w_{u-v} / w_o at each test point was determined from the temperature (and total water content, if necessary.) Then, regression analysis was conducted to determine the relationship between these values and the measured resilient modulus. Data from the thawed, undrained state (assigned to be at a temperature just barely below freezing) were analyzed along with the frozen data.

Thawed/never frozen

For the never frozen and thawed data, the governing parameter in the general form equation (eq 1) was set to be a stress function. The constant K_1 was considered to be a function of the moisture level expressed as the degree of saturation in the sample and, when a range of data were available, the dry density. Thus, the general equation becomes

$$M_r = K_1\left[f(\sigma)\right]^{K_2}, \tag{6}$$

which includes the term

$$K_1 = C_0(S / S_0)^{C_1} \tag{7}$$

or

$$K_1 = C_0(S / S_0)^{C_1}(\gamma_d / \gamma_o)^{C_2} \tag{8}$$

where $f(\sigma)$ is a stress parameter normalized to a unit stress of 6.9 kPa (1.0 lb/in.^{2}); C_o, C_1, and C_2 are constants; S is the degree of saturation, in %; S_o is a unit saturation, 1.0%; γ_d is dry density, in Mg/m^3; and γ_o is a unit density (1.0 Mg/m^3). To conduct the regression analysis, we linearized this equation to form

$$\ln M_r = A_0 + A_1 \ln\left(S / S_0\right) + A_2 \ln\left(\gamma_d / \gamma_o\right) + A_3 \ln\left[f(\sigma)\right]. \tag{9}$$

For a particular set of conditions, then

$$K_1 = e^{A_0}\left(S / S_0\right)^{A_1}\left(\lambda_d / \gamma_o\right)^{A_2} \text{ and } K_2 = A_3.$$

Three stress parameters were investigated to help characterize the stress dependence of the materials tested. These included J_1, the bulk stress (or first stress invariant); τ_{oct}, the octahedral shear stress; and J_2/τ_{oct}, the ratio of the second stress invariant to the octahedral shear stress. In our repeated-load triaxial test, where $\sigma_2 = \sigma_3$ and $\sigma_1 = \sigma_3 + \sigma_d$, the functions are given as:

$$J_1 = 3\sigma_3 + \sigma_d$$

$$\tau_{oct} = \frac{\sqrt{2}}{3}\sigma_d$$

and

$$J_2 / \tau_{oct} = \frac{9\sigma_3^2 + 6\sigma_3\sigma_d}{\sqrt{2}\sigma_d}$$

where $J_1 = \sigma_1 + \sigma_2 + \sigma_3$

$$J_2 = \sigma_1\sigma_2 + \sigma_2\sigma_3 + \sigma_1\sigma_3$$

$$\tau_{oct} = \tfrac{1}{2}\sqrt{(\sigma_1 - \sigma_2)^2 + (\sigma_2 - \sigma_3)^2(\sigma_1 - \sigma_3)^2}.$$

We found that the bulk stress parameter (J_1) provided the best fit to the data for the class 6 special base material. The ratio J_2/τ_{oct} was the stress parameter that best fit the data of the three subbases class 3 special, class 4 special, and class 5 special, and τ_{oct} best characterized the clay subgrades.

We also analyzed the data from the class 6 special base material in the thawed condition using an equation of the form

$$M_r = K_1\, e^{K_2[f(\sigma)]}. \tag{10}$$

As before, K_1 was considered to be a function of the degree of saturation and the dry density (eq 8). In this case, the stress parameter, $f(\sigma)$, was the normalized bulk stress, J_1. This form of the equation was able to accommodate negative stress values that were generated in the layered elastic analysis portion of the predictive model.

RESULTS

General

Appendices A and B give a tabulation of all the laboratory test results of the frozen, thawed, and never-frozen soil specimens. Appendix A contains the data from the current study, which includes the two Mn/ROAD subgrade samples 1206 and 1232, the class 6 special base, and the class 3 special subbase. Appendix B contains the data determined previously from dense graded stone, the substitute for Mn/DOT's class 5 special subbase, and from Albany, New York, taxiway A subbase, the substitute for class 4 special subbase.

Data for the never-frozen 1206 subgrade specimens were acquired on a different testing machine than all the other data. After testing of all specimens was completed, we discovered that this second machine was out of calibration, such that the moduli reported here are much higher than they should be. However, data from the low density (CE 5) samples are close to moduli back-calculated from falling weight deflectometer (FWD) tests on subgrade at the site during fall of 1991.*

Table 6 summarizes the equations that resulted from the regression analysis performed on the data, with the frozen and unfrozen equations given in separate sections. The number "*n*" in Table 6 refers to the number of points evaluated in the analysis. Each stress combination at a given moisture level or temperature results in one data point; thus, the test of a single specimen results in many data points. The table also lists the coefficients of determination (r^2) for these analyses.

Frozen

Figures 4a through 4f illustrate the resilient modulus data vs. temperature for each material in the frozen state. Also shown are the data for the thawed, undrained condition, which are assumed to be valid at a temperature of 0°C and were included as the warmest data point of the regression analyses. Superimposed on the data are lines showing the moduli predicted by the three types of regression equations. Where the predictive equation requires normalization to the total water content, that parameter was set to be the average value for all the specimens tested. For the predictive equation with volumetric unfrozen water, the dry density was also set to be the average value for all the specimens tested.

Figure 4 shows that the frozen modulus does vary primarily as a function of the unfrozen water content. A minor amount of variation results from the various stress combinations acting on the specimens, as shown from the vertical spread in the data at any particular temperature. To illustrate this, Figure 5 shows the data from a few individual deviator stress levels plotted separately for the subgrade samples.

All three types of predictive equations appear to represent the data fairly well. The moduli resulting from the governing parameter, normalized to the total water content, increases less rapidly with decreasing temperature at temperatures just below freezing than do moduli from the other two equations. Unfortunately, the temperature variation of the environmental chamber of the testing machine was too great to allow acquisition of data at temperatures close to the freezing point for the Mn/ROAD materials. When the two substitute materials were tested, a different chamber temperature controlling system was used, and it was possible to obtain data nearer to the freezing point. In these cases, shown in Figures 4d and 4e, the predictive equations without normalization to total water appear to pass nearer to the center of the range of data collected at temperatures warmer than –2.0°C.

Figure 4 also shows that the predictions from the equations whose governing parameters are the gravimetric and volumetric unfrozen water normalized to a unit unfrozen water are not very different. Predictions from the volumetric form rise less rapidly at temperatures just below freezing, while at the colder temperatures, they are slightly larger than the gravimetric form.

*D. Van Deusen, Mn/ROAD, pers. comm. 1992 .

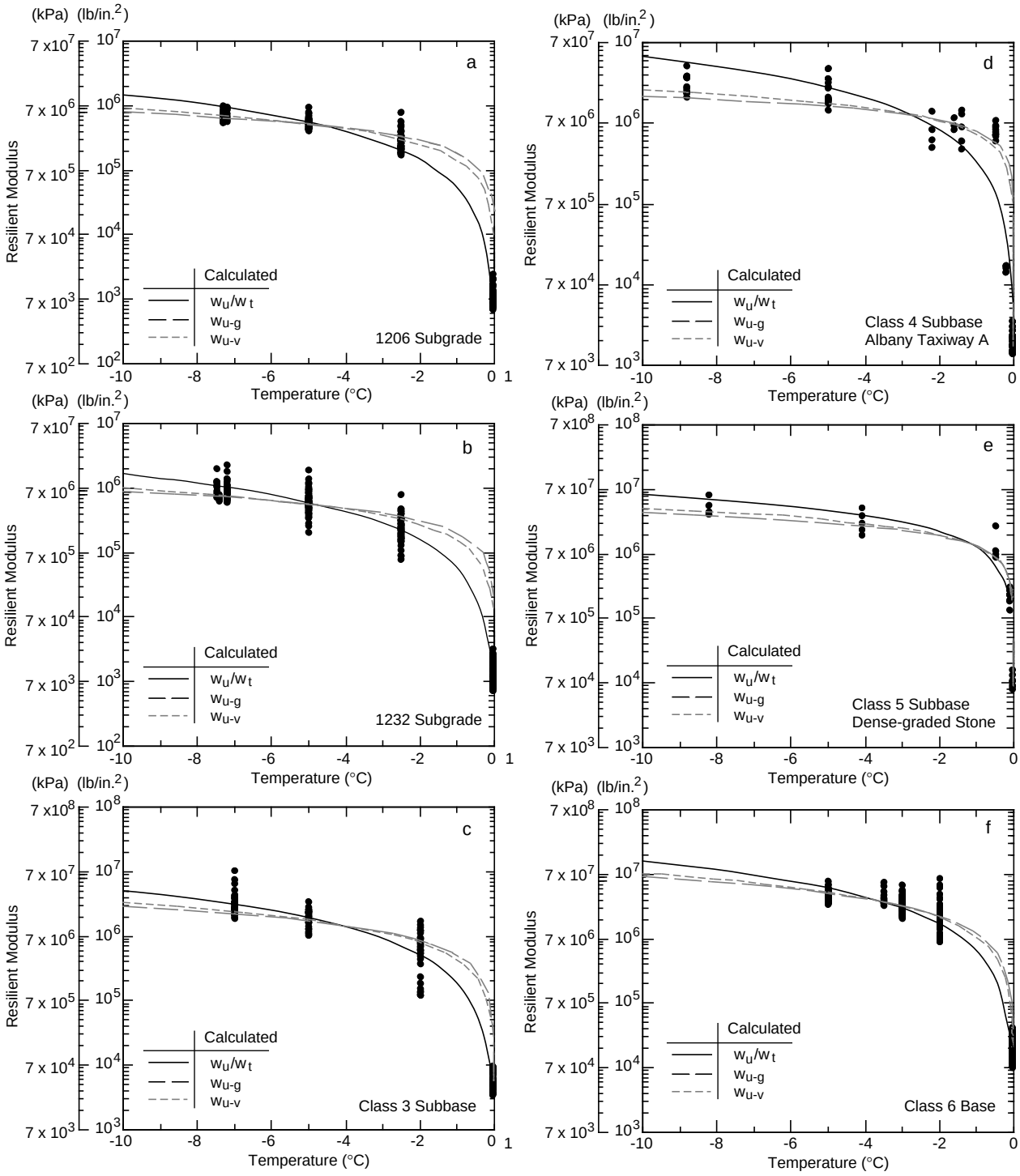

Figure 4. Frozen resilient modulus data vs. temperature. Calculated lines are based on mean total water content or density of all specimens tested, where appropriate.

Table 6. Results of regression analyses—test soils from Mn/ROAD.

A. Frozen condition.

Material	*Equation (M_r in lb/in.^{2})**	n	r^2	*Std error*
Clay subgrade sample 1206 (565)				
Frozen	$M_r = 1,087\, f(w_u)^{-5.259}$	207	0.99	0.319
Frozen	$M_r = 1,049\, f(w_{u-g})^{-2.344}$	207	0.99	0.275
Frozen	$M_r = 1,052\, f(w_{u-v})^{-2.929}$	207	0.99	0.262
Clay subgrade sample 1232 (566)				
Frozen	$M_r = 905\, f(w_u)^{-4.821}$	244	0.98	0.378
Frozen	$M_r = 846\, f(w_{u-g})^{-2.161}$	244	0.98	0.423
Frozen	$M_r = 848\, f(w_{u-v})^{-2.633}$	244	0.98	0.394
Class 3 "stockpile"				
Frozen	$M_r = 5,824\, f(w_u)^{-2.026}$	186	0.97	0.491
Frozen	$M_r = 5,488\, f(w_{u-g})^{-1.076}$	210	0.97	0.507
Frozen	$M_r = 5,542\, f(w_{u-v})^{-1.249}$	186	0.97	0.467
Class 4 (taxiway A subbase)				
Frozen	$M_r = 2,826\, f(w_u)^{-5.220}$	69	0.92	0.835
Frozen	$M_r = 1,813\, f(w_{u-g})^{-1.733}$	85	0.93	0.885
Frozen	$M_r = 1,652\, f(w_{u-v})^{-2.813}$	69	0.91	0.916
Class 5 (dense graded stone)				
Frozen	$M_r = 11,320\, f(w_u)^{-2.036}$	28	0.97	0.404
Frozen	$M_r = 8,695\, f(w_{u-g})^{-1.2814}$	28	0.95	0.511
Frozen	$M_r = 9,245\, f(w_{u-v})^{-1.489}$	28	0.97	0.432
Class 6 "stockpile"				
Frozen	$M_r = 19,924\, f(w_u)^{-1.243}$	260	0.98	0.372
Frozen	$M_r = 19,427\, f(w_{u-g})^{-0.795}$	260	0.98	0.338
Frozen	$M_r = 19,505\, f(w_{u-v})^{-0.897}$	260	0.98	0.341

Notes:
n = number of test points
r^2 = coefficient of determination
M_r = resilient modulus
$f(S) = S/S_o$
S = degree of saturation (%)
S_o = 1.0 %
$f(\gamma) = \gamma_d/\gamma_o$
γ_d = dry density (Mg/m^3)
γ_o = 1.0 Mg/m^3
$f(w_u) = w_{u-g}/w_t$
w_{u-g} = gravimetric unfrozen water content
w_t = gravimetric total water content
$f(w_{u-g}) = w_{u-g}/w_o$
w_o = unit water content (1.0)
$f(w_{u-v}) = w_{u-v}/w_o$
w_{u-v} = volumetric unfrozen water content
σ = stress (lb/in.^{2})
$f_1(\sigma) = J_1/\sigma_o$
$f_2(\sigma) = (J_2/\tau_{oct})/\sigma_o$
$f_3(\sigma) = \tau_{oct}/\sigma_o$
σ_o = 1.0 lb/in.^{2}
J_1 = bulk stress (lb/in.^{2})
$J_1 = 3\sigma_3 + \sigma_d$
J_2 = 2nd stress invariant (lb/in.^{2})
$J_2 = 3\sigma_3^2 + 2\sigma_3\sigma_d$
τ_{oct} = octahedral shear stress (lb/in.^{2})
$\tau_{oct} = \left(\sqrt{2}/3\right)\sigma_d$

*Output from equations can be converted to kilopascals through multiplying by 6.895

Table 6 (cont'd). Results of regression analyses—test soils from Mn/ROAD.

B. Unfrozen condtion

Material	*Equation (M_r in lb/in.^{2})**	n	r^2	*Std error*
Clay subgrade sample 1206 (565)				
Never frozen	$M_r = 1{,}597{,}000\, f(S)^{-2.63}\, f(\gamma)^{14.42}\, f_3(\sigma)^{-0.257}$	655	0.82	0.251
Clay subgrade sample 1232 (566)				
Never frozen	$M_r = 1.518\times10^{30}\, f(S)^{-13.85}\, f_3(\sigma)^{-0.272}$	451	0.95	0.328
Class 3 "stockpile"				
Thawed	$M_r = 283{,}300\, f(S)^{-1.003}\, f_2(\sigma)^{0.206}$	408	0.86	0.520
Class 4 (taxiway A subbase)				
Thawed	$M_r = 8.946\times10^{8}\, f(S)^{-3.026}\, f_2(\sigma)^{0.292}$	149	0.86	0.168
Class 5 (dense graded stone)				
Thawed	$M_r = 382{,}400\, f(S)^{-0.8759}\, f_2(\sigma)^{0.1640}$	64	0.77	0.164
Class 6 "stockpile"				
Thawed	$M_r = 1{,}391\, f(S)^{-0.507}\, f(\gamma)^{4.04}\, f_1(\sigma)^{0.608}$	492	0.79	0.232
Thawed	$M_r = 5{,}257\, f(S)^{-0.486}\, f(\gamma)^{4.05} e^{0.0193 f_1(\sigma)}$	492	0.76	0.249

*Output from equations can be converted to kilopascals through multiplying by 6.895

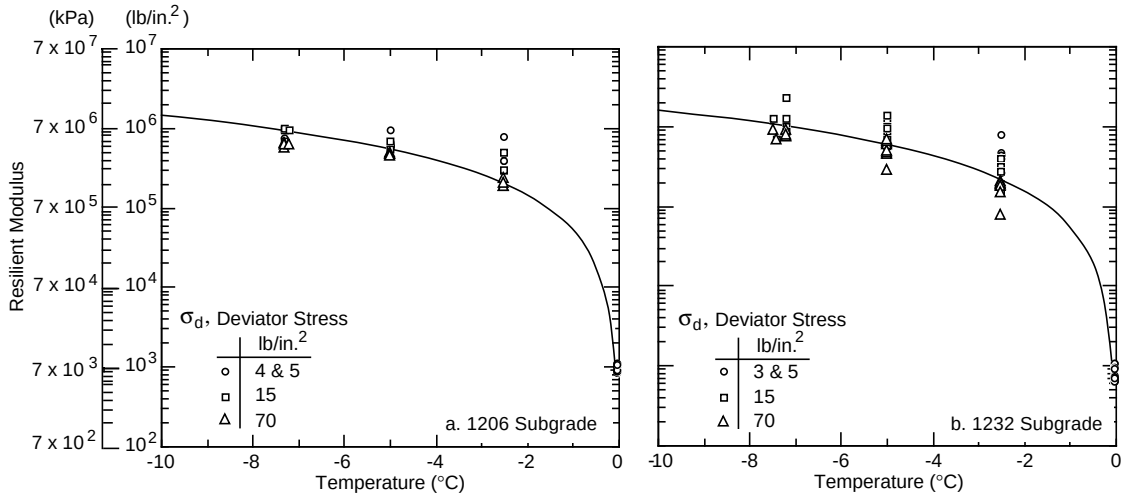

Figure 5. Effect of stress on frozen resilient modulus.

Figure 6 compares the modulus vs. temperature for all the frozen Mn/DOT materials predicted from the regression equations in Table 6, with the governing parameters w_{u-g}/w_t and w_{u-v}. At any given temperature, the subgrade specimens have the lowest moduli. In general, the base and subbase moduli increase with decreasing amounts of fines in the material. The curve for the class 5 special material has a slightly different shape than the rest, which is probably related to the estimated choice of coefficients for the distribution of unfrozen water content with temperature.

Unfrozen

Figures 7a through 7f show the resilient modulus data vs. degree of saturation for the unfrozen specimens. For the two subgrade materials, data are from specimens that were never frozen, and data from the base/subbase materials are from specimens that were thawed subsequent to freez-

ing. Also shown is a line representing the predicted moduli resulting from the equations given in Table 6, at the mean stress level tested. Where dry density is included in the equation, it was set at the average value of all specimens tested. It can be seen in Figures 7a through 7f that moisture level does influence the unfrozen moduli, but to different degrees, depending on the material.

The vertical spread in the data points at a particular degree of saturation (Fig. 7) is the result of the materials response to the different stress combinations applied (Table 3a). In the case of the 1206 subgrade and the class 6 special base, it also relates to the variation in density. To show the influence of density in the 1206 subgrade data, Figure 8 differentiates the data from three density ranges (high, medium, and low), along with the corresponding predicted resilient moduli lines. Note that the low density moduli are most representative of moduli back-calculated from FWD deflections measured on site at Mn/ROAD.

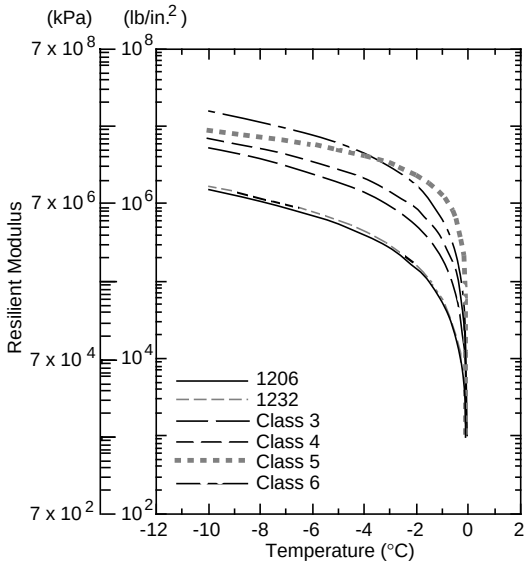

a. Governing parameter w_{u-g}/w_t.

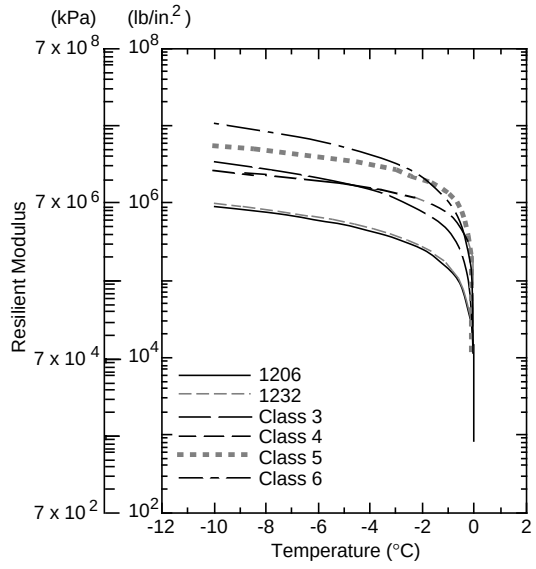

b. Governing parameter w_{u-v}.

Figure 6. Predicted frozen resilient modulus for all Mn/ROAD materials.

The effect of stress combinations is shown in Figure 9 for the low-density 1206 subgrade data, and all of the 1232 subgrade and class 3 special subbase data. The two subgrades display an inverse relationship between modulus and deviator stress; the class 3 special subbase has a proportional relationship between modulus and the stress parameter J_2/τ_{oct}.

Figure 10 demonstrates the relative influence of the deviator stress and confining pressure (σ_3) on the modulus of a single 1206 subgrade specimen at 16.1% water content. The deviator stress has the major influence, while confining pressure produces only minor variations in the moduli. The figure also includes a line of predicted resilient moduli based on a regression analysis of these data alone, in the form:

$$M_r \text{ (lb/ft}^2) = K_1 (\sigma_d)^{K_2},$$

as well as the upper and lower 95% confidence interval around the mean line. The confidence band brackets the variation in modulus related to σ_3.

We generated several predicted curves for individual samples as described above to isolate the influence of moisture content and density, respectively, on the resilient modulus of the 1206 subgrade material. Figure 11 shows the relationship between modulus and deviator stress of specimens with a similar density, but with different moisture levels. It confirms the expected relationship that the drier sample exhibits a higher modulus at similar stress conditions. Figure 12 compares two samples with similar moisture, showing that the higher density sample has higher moduli.

A comparison of the predicted modulus curves generated by the equations in Table 6 for all the materials studied is given in Figure 13. Among the curves of the base/subbase materials, there is a general increase in the predicted moduli as the

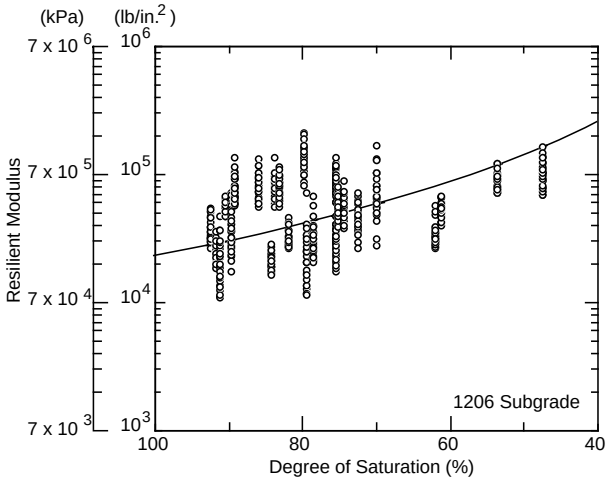

a. 1206 subgrade. (These data are probably in error—see text.)

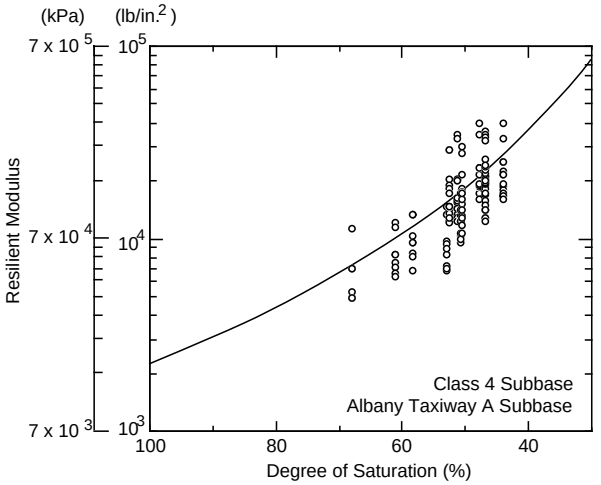

d. Class 4 special subbase.

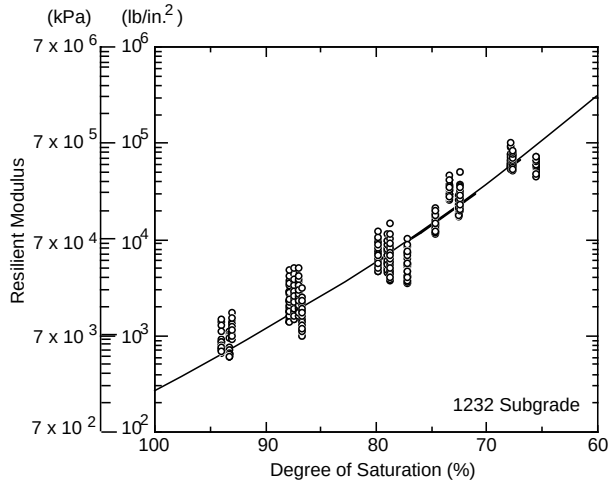

b. 1232 subgrade.

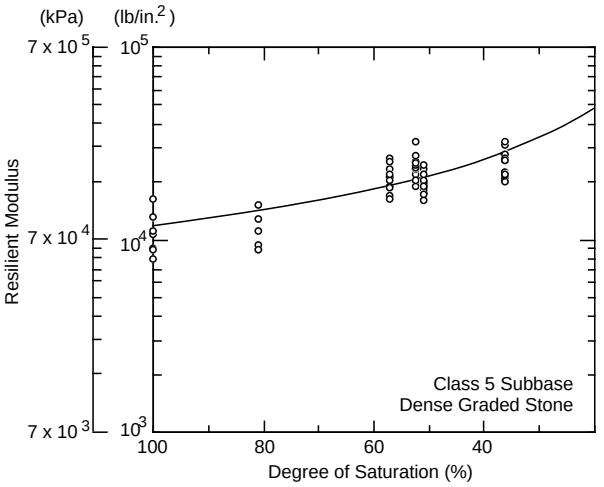

e. Class 5 special subbase.

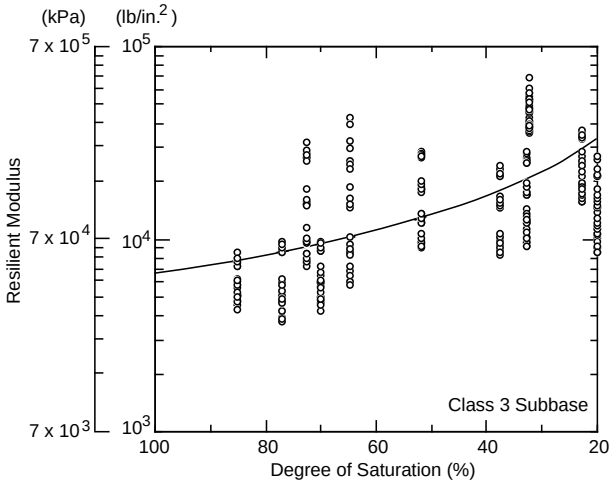

c. Class 3 special subbase.

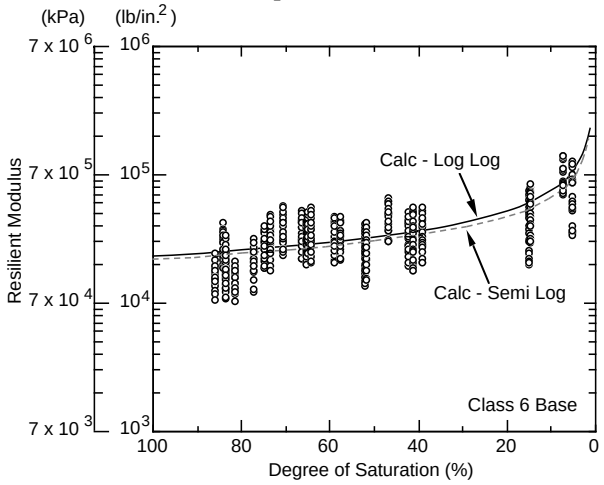

f. Class 6 special base.

Figure 7. Resilient modulus vs. degree of saturation for never frozen subgrade materials and thawed base/subbase materials. Solid line represents calculated value based on mean condition of stress (and density where included).

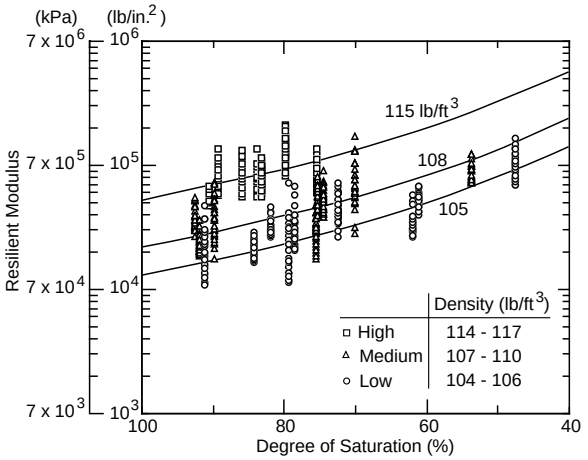

Figure 8. Resilient modulus vs. degree of saturation of never-frozen 1206 subgrade material illustrating the effect of dry density.

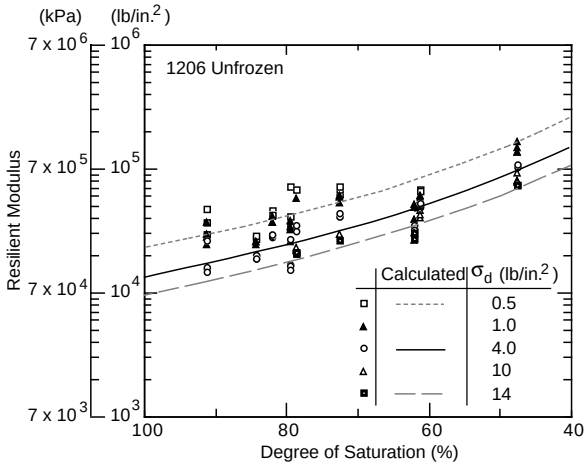

a. Low-density (1.66–1.7-Mg/m^3 or 104–106-lb/ft^3) 1206 subgrade. (These data are probably in error—see text.)

amount of fines in the material decreases, with the exception of the class 4 special material. There is also a decrease in the slope of the predicted curves with decreasing fine content, indicating the expected lesser influence of moisture content on the moduli of the coarser materials. The curves of the two clay subgrades depart somewhat from this pattern. The curve for the 1232 subgrade has an extremely steep slope, showing a much stronger influence of the degree of saturation on the modulus. The curve of predicted moduli for the 1206 subgrade is higher than those for the coarser materials. Although this is contrary to conventional rules-of-thumb, high moduli for cohesive materials have also been reported by Robnet and Thompson (1973). However, it is more likely that the high 1206 subgrade moduli are related to the miscalibration of the testing machine. This possibility is being investigated in more detail and findings will be included in the Phase 2 report (Berg in prep.).

For each material tested, Figure 14 shows the frozen and thawed/unfrozen moduli data points and curves based on the regression equations resulting from this analysis. Data in Figure 14 illustrate the rapid increase in modulus as the soils freeze and a lower-magnitude increase in modulus values with decreasing saturation. To illustrate these general trends, the calculated relationships vs. degree of saturation are also shown, for one stress condition only. As shown in Figure 9, stress conditions also influence resilient modulus values.

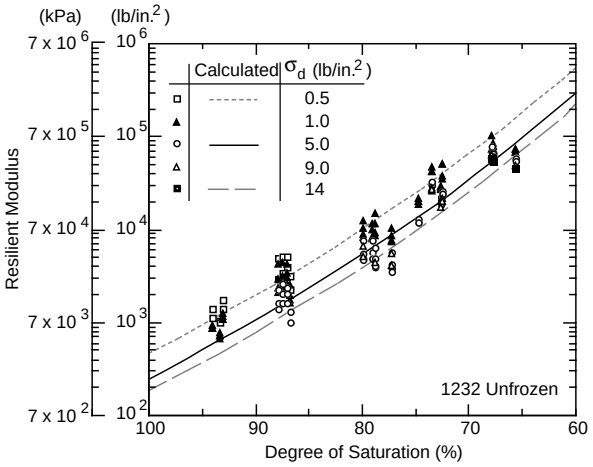

b. 1232 subgrade.

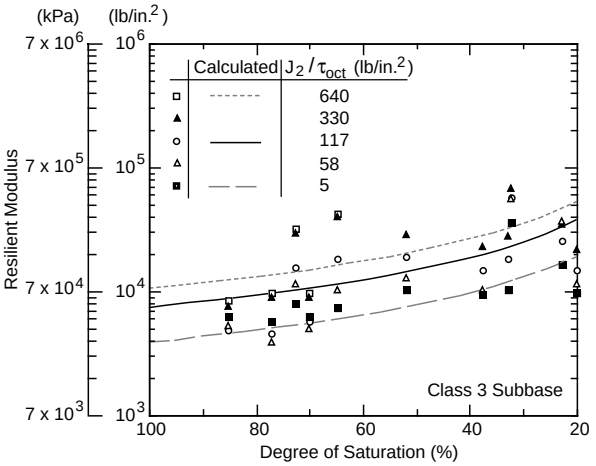

c. Class 3 special subbase.

Figure 9. Resilient modulus vs. degree of saturation illustrating effect of stress parameters.

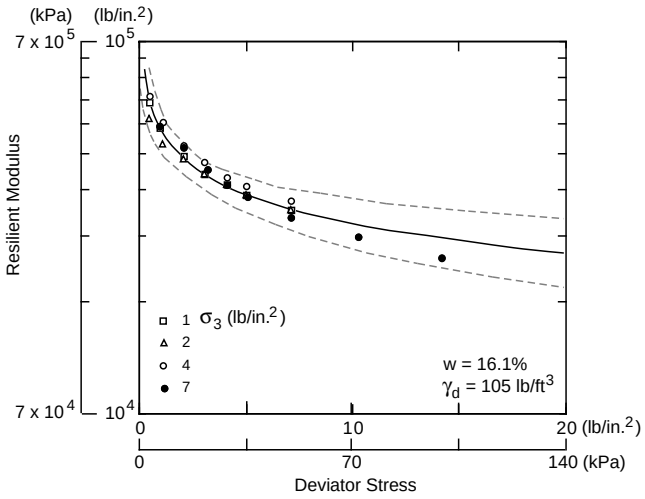

Figure 10. Resilient modulus vs. deviator stress applied to a single 1206 subgrade specimen. Data points illustrate level of confining stress applied. Dashed lines indicate band of 95% confidence interval.

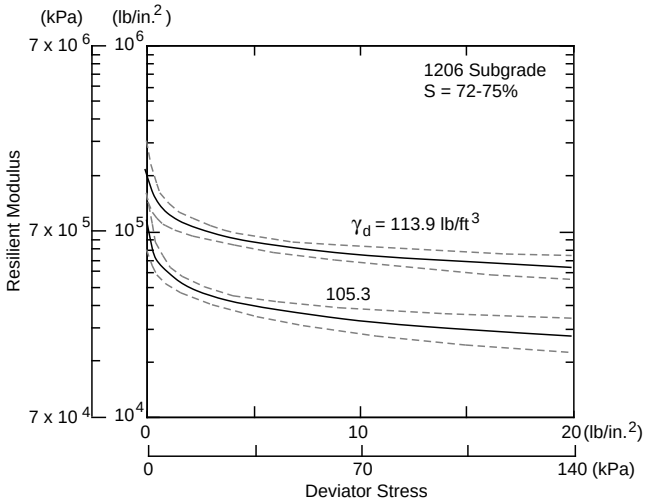

Figure 12. Resilient modulus vs. deviator stress applied to two 1206 subgrade specimens illustrating effect of dry density. Dashed lines indicate band of 95% confidence interval.

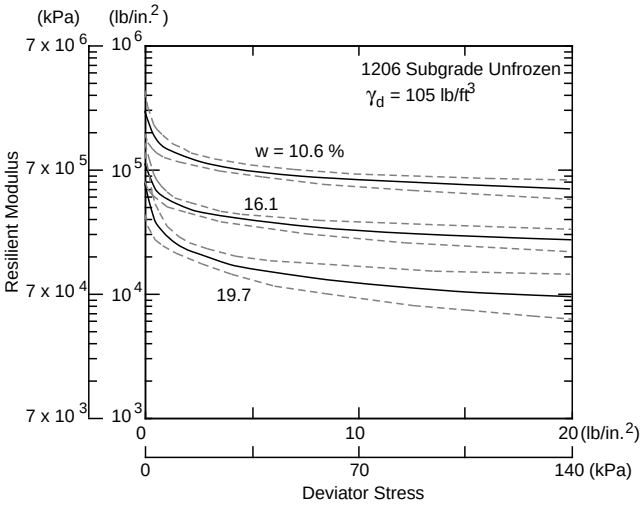

Figure 11. Resilient modulus vs. deviator stress applied to three 1206 subgrade specimens illustrating effect of moisture condition. Dashed lines indicate band of 95% confidence interval.

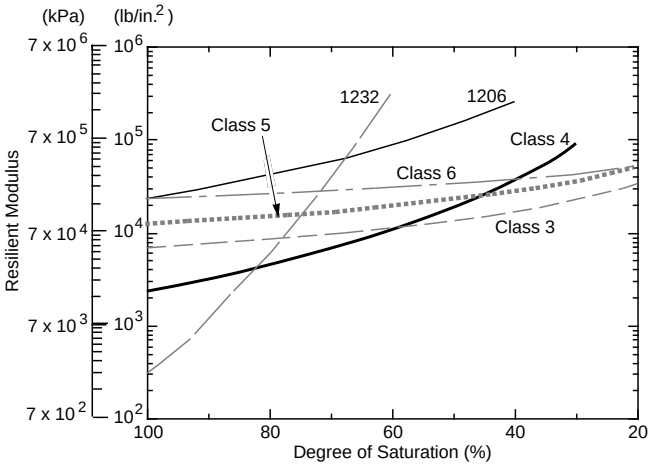

Figure 13. Predicted moduli for all materials in unfrozen condition.

A significant discontinuity between thawed 0°C and 100% saturated modulus values is shown in Figure 14a. As indicated previously, the difference is probably due to miscalibration of the testing equipment for the unfrozen data rather than an actual large difference in resilient modulus values at these points. These data are currently being reexamined and findings will be reported in the Phase 2 report (Berg in prep.).

For the granular base and subbase materials, essentially no discontinuity is apparent between the modulus of the thawed, 0°C material and the same material at 100% saturation.

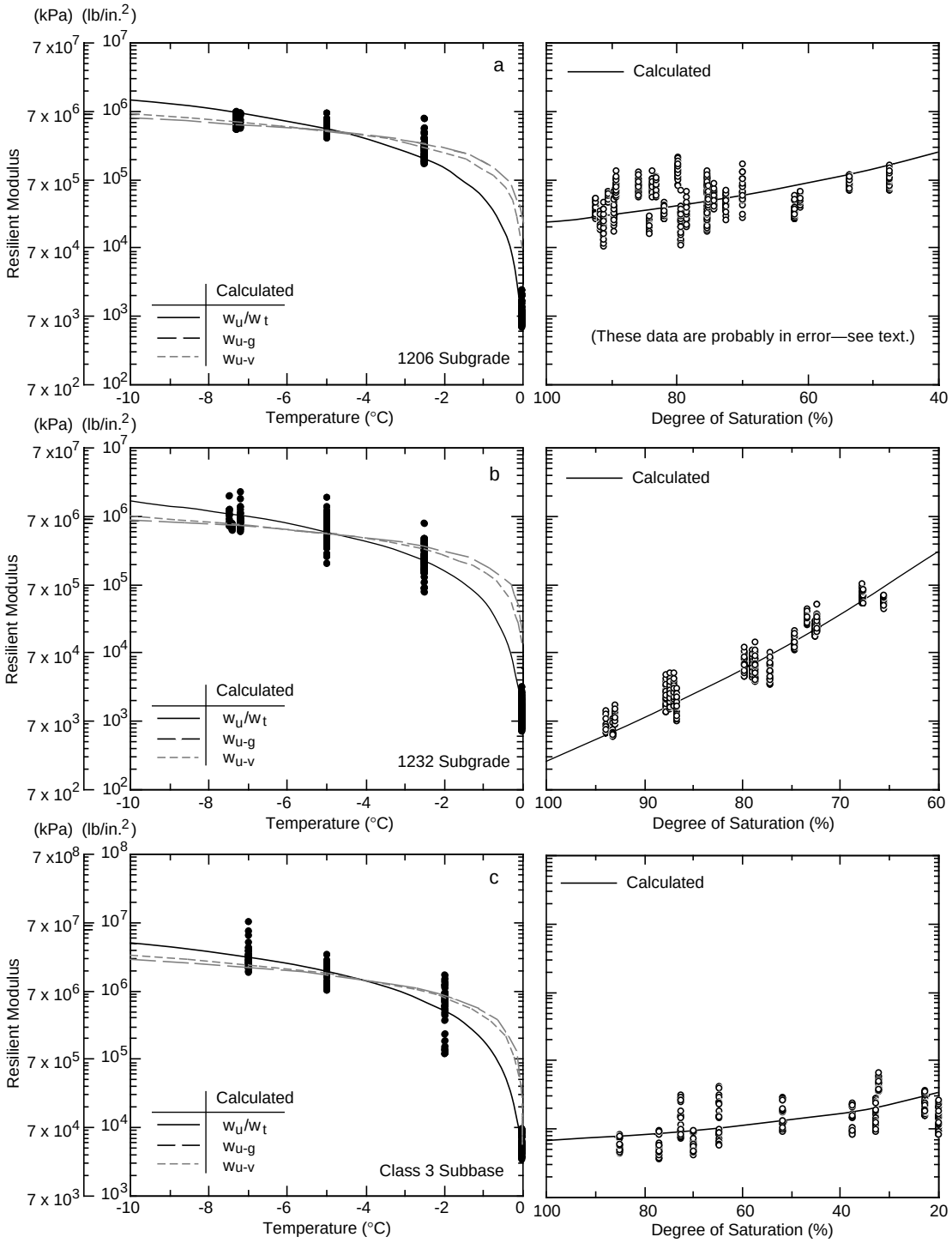

Figure 14. Comparison of frozen and unfrozen modulus data.

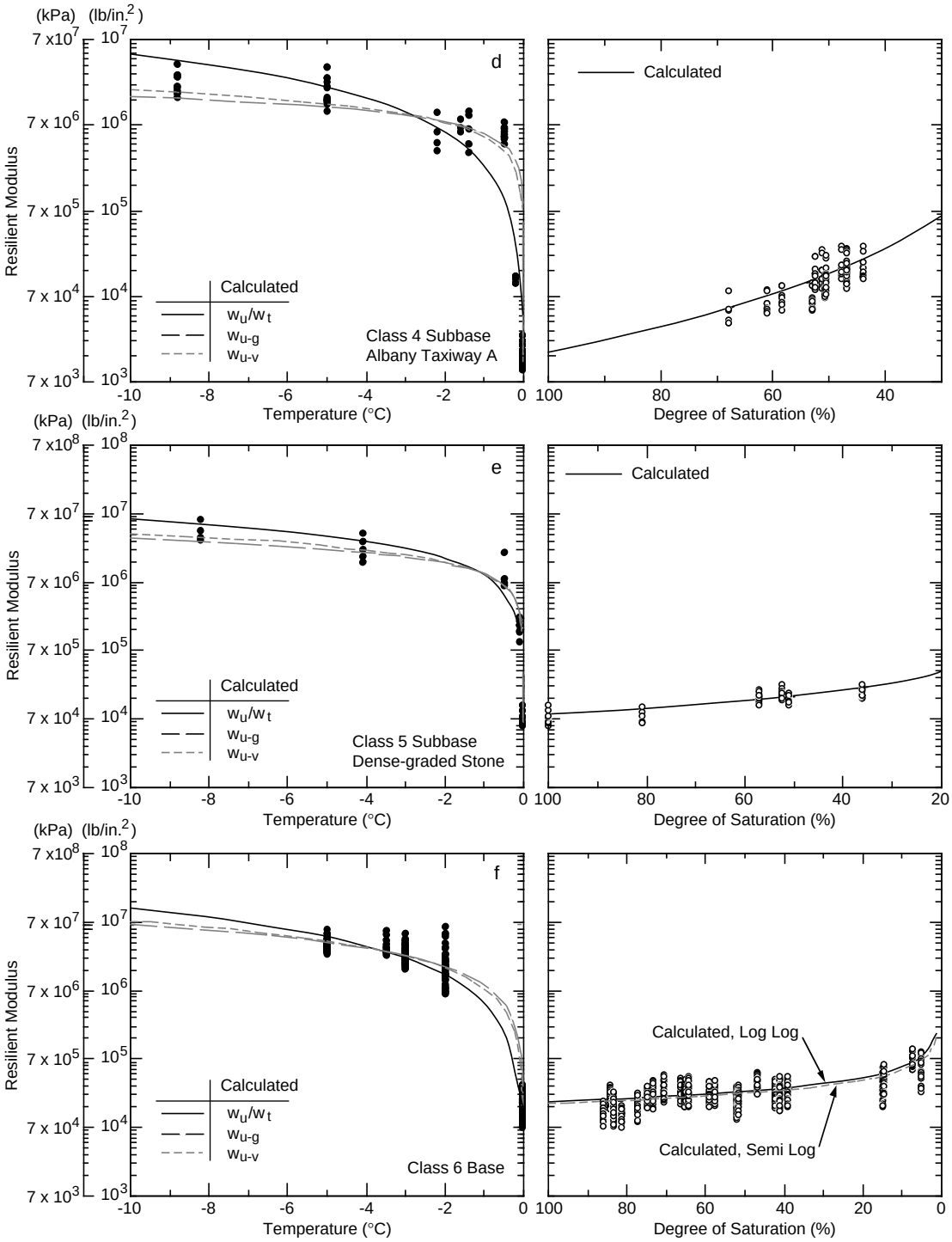

Figure 14 (cont'd).

CONCLUSIONS

Laboratory resilient modulus tests on the Mn/ROAD unbound base and subgrade materials have resulted in the following:

1. All materials exhibited a two to three order of magnitude increase in resilient modulus at subfreezing temperatures of –2°C and lower.
2. All of the materials exhibited an increase in modulus as the degree of saturation decreased.
3. The modulus value of all of the materials was stress dependent.
4. For the highly frost-susceptible 1206 subgrade and the class 6 special base course, the resilient modulus was also dependent on the density of the sample tested. We did not test samples at a wide variety of densities for the other materials, but density probably impacts modulus values of those materials also.

LITERATURE CITED

Berg, R.L. (in prep.) Resilient modulus testing of materials from Mn/ROAD, Phase 2. USA Cold Regions Research and Engineering Laboratory, Special Report.

Bigl, S.R. and R.L. Berg (1996a) Testing of materials from the Minnesota Cold Regions Pavement Research Test Facility. USA Cold Regions Research and Engineering Laboratory, Special Report 96-20, Mn/DOT Report 96-24.

Bigl, S.R. and R.L. Berg (1996b) Modeling of Mn/ROAD test sections with the CRREL mechanistic pavement design procedure. USA Cold Regions Research and Engineering Laboratory, Special Report 96-21, Mn/DOT Report 96-22.

Bigl, S.R. and R.L. Berg (1996c) Material testing and initial pavement design modeling: Minnesota Road Research Project. USA Cold Regions Research and Engineering Laboratory, CRREL Report 96-14, Mn/DOT Report 96-23.

Chamberlain, E.J. (1987) A freeze thaw test to determine the frost susceptibility of soils. USA Cold Regions Research and Engineering Laboratory, CRREL Special Report 87-1.

Cole, D.M., G.D. Durell and E.J. Chamberlain (1985) Repeated load triaxial testing of frozen and thawed soils. *Geotechnical Testing Journal*, **8**(4): 166–170.

Cole, D.M., D. Bentley, G.D. Durell and T. Johnson (1986) Resilient modulus of freeze-thaw affected granular soils for pavement design and evaluation. Part 1. Laboratory tests on soils from Winchendon, Massachusetts, test sections. USA Cold Regions Research and Engineering Laboratory, CRREL Report 86-4.

Cole, D.M., D. Bentley, G.D. Durell and T. Johnson (1987) Resilient modulus of freeze-thaw affected granular soils for pavement design and evaluation. Part 3. Laboratory tests on soils from Albany County Airport. USA Cold Regions Research and Engineering Laboratory, CRREL Report 87-2.

Robnet, Q.L., and M.R. Thompson (1973) Interim report—Resilient properties of subgrade soils—Phase 1. Development of testing procedure. Transportation Engineering Series 5, Illinois Cooperative Highway Research Program Series 139, University of Illinois, Urbana, Illinois, May.

APPENDIX A: Mn/ROAD MATERIALS RESILIENT MODULUS TEST RESULTS

[The paper version of this report includes 64 pages of data that are not reproduced here. Paper copies are available through the National Technical Information Service. See the inside cover of this report for ordering information.]

APPENDIX B: SUBSTITUTE MATERIALS RESILIENT MODULUS TEST RESULTS

[The paper version of this report includes nine pages of data that are not reproduced here. Paper copies are available through the National Technical Information Service. See the inside cover of this report for ordering information.]

REPORT DOCUMENTATION PAGE

Form Approved
OMB No. 0704-0188

1. AGENCY USE ONLY (Leave blank)	2. REPORT DATE	3. REPORT TYPE AND DATES COVERED
	September 1996	Final Report June 1990–October 1991

4. TITLE AND SUBTITLE

Resilient Modulus Testing of Materials from Mn/ROAD, Phase 1

5. FUNDING NUMBERS

CPAR Project
Agreement No. 64632
Task Order No. 1

6. AUTHORS

Richard L. Berg, Susan R. Bigl, Jeffrey A. Stark and Glenn D. Durell

7. PERFORMING ORGANIZATION NAME(S) AND ADDRESS(ES)

U.S. Army Cold Regions Research and Engineering Laboratory
72 Lyme Road
Hanover, New Hampshire 03755-1290

8. PERFORMING ORGANIZATION REPORT NUMBER

Special Report 96-19

9. SPONSORING/MONITORING AGENCY NAME(S) AND ADDRESS(ES)

Minnesota Department of Transportation
395 John Ireland Boulevard Mail Stop 330
St. Paul, Minnesota 55155

10. SPONSORING/MONITORING AGENCY REPORT NUMBER

MN/RC-96/21

11. SUPPLEMENTARY NOTES

For conversion of SI units to non-SI units of measurement consult ASTM Standard E380-93, *Standard Practice for Use of the International System of Units*, published by the American Society for Testing and Materials, 1916 Race St., Philadelphia, Pa. 19103.

12a. DISTRIBUTION/AVAILABILITY STATEMENT

Approved for public release; distribution is unlimited.

Available from NTIS, Springfield, Virginia 22161

12b. DISTRIBUTION CODE

13. ABSTRACT (*Maximum 200 words*)

The U.S. Army Cold Regions Research and Engineering Laboratory (CRREL) conducted resilient modulus tests on materials from the Mn/ROAD test site for the Minnesota Department of Transportation. Materials tested included samples of the lean clay subgrade at the site and the two extreme grades of base designed specifically for Mn/ROAD. Some specimens were tested in both frozen and subsequently "thawed" conditions; others were tested at room temperature without ever having been frozen. Researchers performed linear regression analysis on the data to develop equations that predict frozen modulus based on unfrozen water content and unfrozen modulus based on stress, degree of saturation and density. We also reanalyzed data from two previously tested materials. CRREL can use the study's equations in the Mechanistic Pavement Design and Evaluation Procedure under development at CRREL to predict estimated damage in some Mn/ROAD test sections.

14. SUBJECT TERMS		15. NUMBER OF PAGES
Cold regions subgrades and bases Mechanistic Pavement Design and Evaluation Procedure	Resilient modulus	103
		16. PRICE CODE

17. SECURITY CLASSIFICATION OF REPORT	18. SECURITY CLASSIFICATION OF THIS PAGE	19. SECURITY CLASSIFICATION OF ABSTRACT	20. LIMITATION OF ABSTRACT
UNCLASSIFIED	UNCLASSIFIED	UNCLASSIFIED	UL